Supplementary Appendix

This appendix has been provided by the authors to give readers additional information about their work.

Supplement to: Jamuar SS, Lam A-TN, Kircher M, et al. Somatic mutations in cerebral cortical malformations. N Engl J Med 2014;371:733-43. DOI: 10.1056/NEJMoa1314432

SUPPLEMENTARY APPENDIX

Deep sequence analysis of the role of somatic mutations in cerebral cortical malformations

Table of contents

Brain Malformation Study Group

- Christopher A. Walsh*, PI
- Annapurna Poduri*
- Mustafa Sahin*
- Bernard S. Chang*
- Timothy W. Yu*
- Saumya S. Jamuar*
- Meral Topcu*
- Dina Amrom*
- Eva Andermann*
- Renzo Guerrini*
- Ingrid E. Scheffer*
- Samuel F. Berkovic*
- Richard J. Leventer*
- A James Barkovich*
- Bernard Dan*
- Elena Parrini*
- Ganeshwaran Mochida, Division of Genetics and Genomics, Boston Children's Hospital, Boston, MA, USA
- Heather Olson, Division of Neurology, Boston Children's Hospital, Boston, MA, USA
- Joseph G. Gleeson, Dept. of Neurosciences and Pediatrics, University of California, San Diego, CA, USA

- William Dobyns, Division of Genetic Medicine, University of Washington, Seattle, WA, USA
- John Mulley, Royal Children's Hospital, The University of Melbourne, Australia
- Michel Berg, Department of Neurology, University of Rochester Medical Center, Rochester, New York, USA
- Z Yapici, Department of Neurology, Division of Child Neurology, Istanbul Faculty of Medicine, Istanbul University, Istanbul, Turkey
- Nehama Kfir, Department of Neurology, Division of Child Neurology, Istanbul Faculty of Medicine, Istanbul University, Istanbul, Turkey
- Sangeeta Dey, 594 Marrett Road, Suite 22, Lexington, MA, USA
- Adre J. DuPlessis, Children's National Medical Center, Center for Neuroscience Research (CNR), Washington, DC, USA
- James Wheless, Department of Pediatric Neurology, The University of Tennessee Health Science Center, Pediatric Neurology, Memphis, TN, USA
- Jean Ricci Goodman, Maternal/Fetal Medicine 2160 S. First Ave., Maywood, IL, USA
- Elizabeth Butler, Michigan State University, Department of Pediatrics and Human Development, East Lansing, MI, USA
- Grace Yoon, Division of Clinical and Metabolic Genetics, The Hospital for Sick Children, Toronto, Canada
- Alva Moncayo, Servicio de Neurología Pediátrica, Hospital General Médico Nacional La Raza, México DF, Mexico
- John N. Gaitanis, Dept of Neurology, Hasbro Children’s Hospital, Providence, RI, USA
- Tzipora Falik Zaccai, Institute of Human Genetics, Bar-Ilan University, Israel

- Kazuhiro Kamuro, Department of Pediatrics, Kokubu Seikyo Hospital, Kogoshima, Japan

***for affiliations of these authors, please refer to the title page**

The study was initiated in May 2012 and completed in Nov 2013.

Supplementary text

Methods

Gene selection: Candidate genes were selected based on findings from whole exome studies and RNA-Seq analysis of the developing mouse and human cerebral cortex[1], with emphasis on genes encoding microtubule subunits and dynein/kinesin motors that are highly expressed during human cerebral cortex development.

Controls: Five samples from patients (Table S2) with known mutations were included in our analyses as positive controls. In addition, to determine the sensitivity of our variant calling for low-level somatic mosaicism, we generated a series of mosaic control samples by diluting DNA from two individuals known to carry heterozygous mutations in either *DCX* or *FLNA* with DNA from an individual without *DCX* and *FLNA* mutations to generate mutant allele frequencies of 50%, 10%, 1% and 0.1%.

Targeted sequencing: Library preparation was performed as per manufacturer's protocol. Pooled oligonucleotides were used to capture target exons from 250 ng of leukocyte-derived DNA from each proband. PCR was performed using universal primers, with the introduction of unique 8-base barcodes on both ends. Pooled libraries were subjected to massively parallel sequencing using a 251-bp paired-end protocol on the MiSeq platform.

Data analysis, variant calling, and Sanger validation: Raw read data processing and mapping were performed using BWA-SW[2]. Single nucleotide variant (SNV) and insertion and/or deletion (indel) calling and filtering were performed using GATK[3]. Variants were quality filtered to exclude false positives according to standard thresholds (QUAL<30, QD<5, coverage<10x and clustered variants (window size of 10). Variant annotations were applied with MiSeq Reporter version 2.1.43 using the Somatic Variant Caller[4]. Data from the Exome sequencing project

(ESP)[5], dbSNP 137[6] and 1000 Genomes Project[7] were used to assess variant frequencies in control population.

Results

CONFIRMATION AND IDENTIFICATION OF ADDITIONAL CANDIDATE GENES

Individual LIS-6801 with posterior pachygyria, diminished white matter and abnormal corpus callosum (Figure S7) showed a previously unreported variant in *KIF5C* (A268S) (Table S5), a gene that was recently identified in a family which included 4 affected boys with severe malformations of cortical development and microcephaly[10]. *KIF5C* encodes a member of the kinesin superfamily involved in intracellular transport along microtubules[10]. Though we were unable to perform segregation as parental DNA was unavailable, this variant alters a highly conserved residue in the kinesin motor domain, and was predicted to be pathogenic and was absent from the control population. Therefore, this likely mutation further supports a role of *KIF5C* in cerebral cortical malformations.

We found variants in three candidate genes for neuronal migration disorders that bear further study— *KIF7* (G94D), *KIF1A* (R18W) and *KIF26A* (Q455R) in individuals BFP-801, PAC-1701 and DC-7801, respectively (Table S5). As parental DNA was unavailable for PAC-1701 and DC-7801, we were unable to perform segregation analysis. Follow-up segregation analysis by Sanger sequencing revealed that father of BFP-801 had a minor peak consistent with mosaicism (Figure S8), which was confirmed on subcloning (2 out of 16 reads, data not shown). Heterozygous mutation in *KIF7* has been associated with developmental delay[11]. Biallelic mutations in *KIF7* have been associated with acrocallosal syndrome and hydrolethalus, while heterozygous mutations in *KIF7* interact with other ciliary genes to exacerbate overall severity in Bardet-Biedl syndrome[12]. Review of published MRIs shows widespread gyral abnormalities with *KIF7* mutations[12]. Her MRI showed bilateral frontal, temporal, and parietal pachygyria. The *KIF1A* mutation in individual PAC-1701 affects a highly conserved amino acid in the kinesin

motor domain. Doublecortin (encoded by *DCX* and associated with neuronal migration disorders*)* is essential for KIF1A function[13], and a mutation in the kinesin motor domain may affect the doublecortin-KIF1A interaction resulting in a similar phenotype. Indeed, MRI (Figure S9) of this individual showed frontal pachygyria, as well as a thick corpus callosum and moderately reduced white matter volume. Missense mutation in *KIF1A* has also been reported in an individual with intellectual disability and mild cerebellar vermian atrophy[14]. The *KIF26A* mutation in individual DC-7801 affects a highly conserved nucleotide in the kinesin motor domain. His MRI (Figure S10) showed subcortical band heterotopia. Human mutations in *KIF26A* have not been reported previously. *KIF26A* encodes a kinesin protein that is involved in the microtubule network and has been implicated in enteric neuronal development[15].

Figure S1: Schematic workflow of our targeted deep sequencing

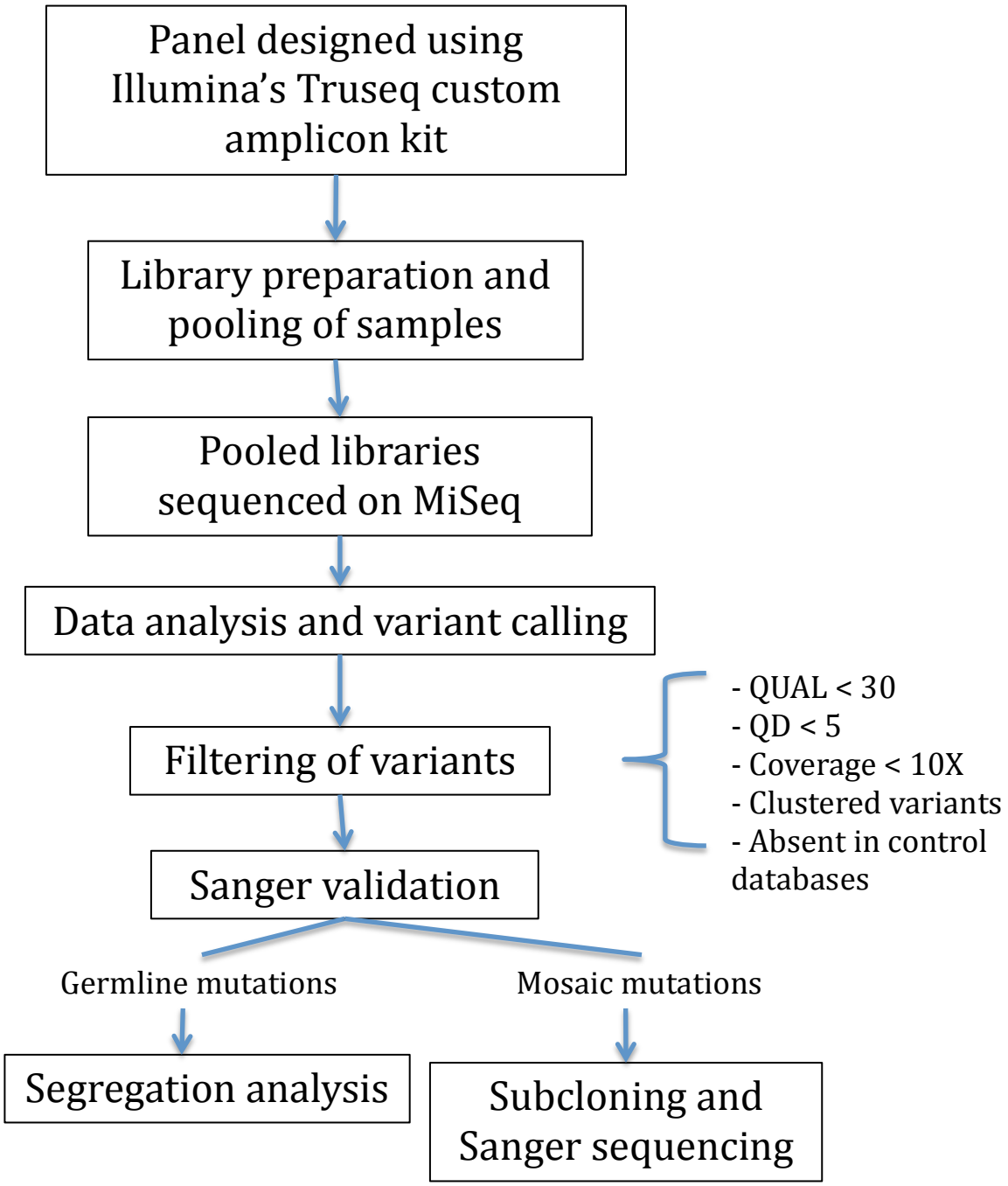

Figure S2: Estimated *p* value for differing AARF at different depths of coverage.
As the read depth increases, the probability of correctly calling a mosaic variant increases. The read depth required is dependent on the AARF. For e.g. for AARF ≤30%, the required read depth is ≈300x and for AARF ≤40%, the required read depth increases exponentially to 1000x. The y-axis represents negative log *p* value and hence a higher number corresponds to a smaller p value. Dashed line denotes the threshold of significant *p* value

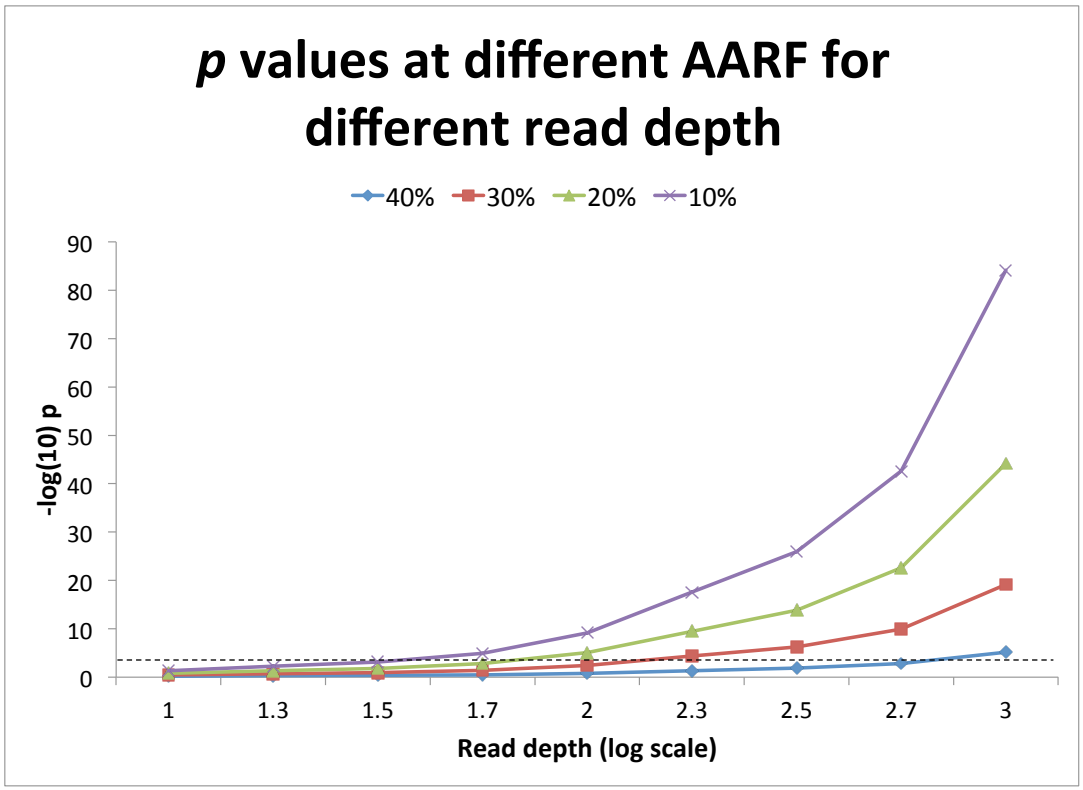

Figure S3: Calibration sample
Screenshot of Integrative Genomic Viewer shows that deep sequencing on calibration sample with germline DCX mutation (c.115C>T;p.R39X) mixed with wild type allele at varying proportions was detected at a threshold of 1% mosaicism.

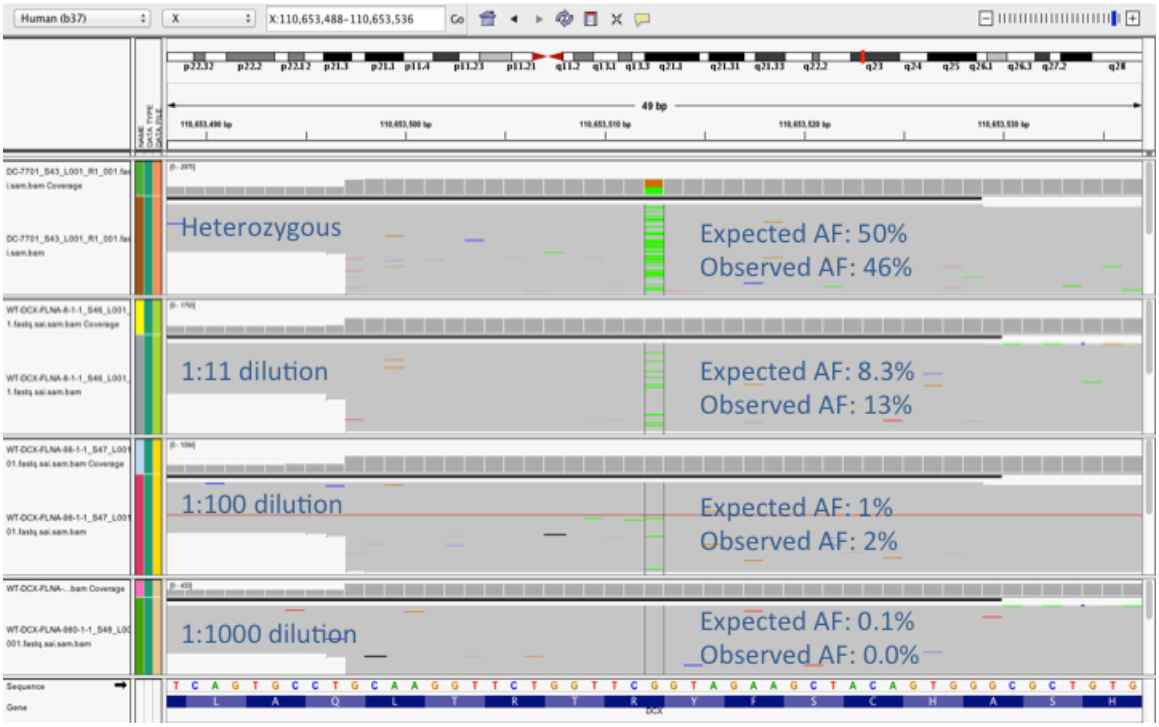

Figure S4: Sanger chromatogram of PH-16001.
The variant (delG) was reported at an allele fraction of 35% on NGS, but appeared as heterozygous germline variant on Sanger sequencing. However, subcloning confirmed the mutation to be mosaic (reference allele in 118 colonies, mutant allele in 67 colonies, allele fraction 36%, *p*=0.0086)

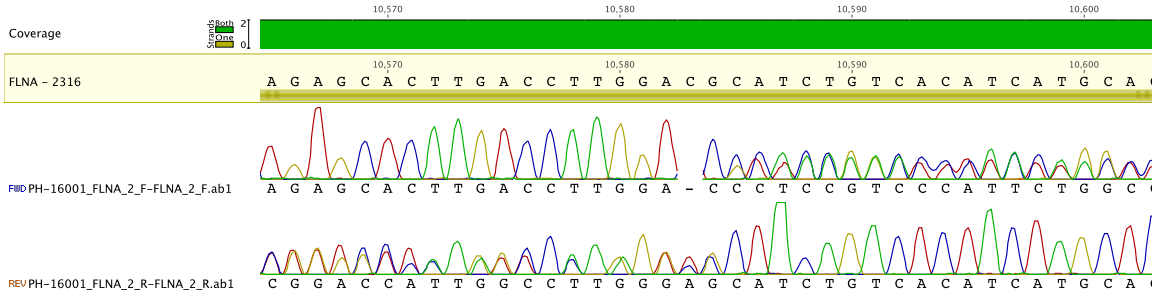

Figure S5: A comparison of synonymous and rare protein-altering mutations across the three phenotypes. Synonymous variants in genes associated with a particular phenotype were equally distributed across each phenotype (numbers within each bar represent the average number of variants called per gene group per sample), while rare protein-altering pathogenic variants in the same genes were specifically associated with the phenotype they are known to cause, showing the specificity of pathogenic variants to diagnosis. DC related genes= *DCX, LIS1, ARX, TUBA1A, TUBB2B, TUBB3*; PVNH related gene= *FLNA*; PMG-M related genes= *AKT3, PIK3CA, PIK3R2*. **variant in *PIK3R2* is a rare protein altering variant that was predicted to be pathogenic by *in silico* prediction software. However, it was inherited from an unaffected parent and is unlikely to be causative (Table S6).

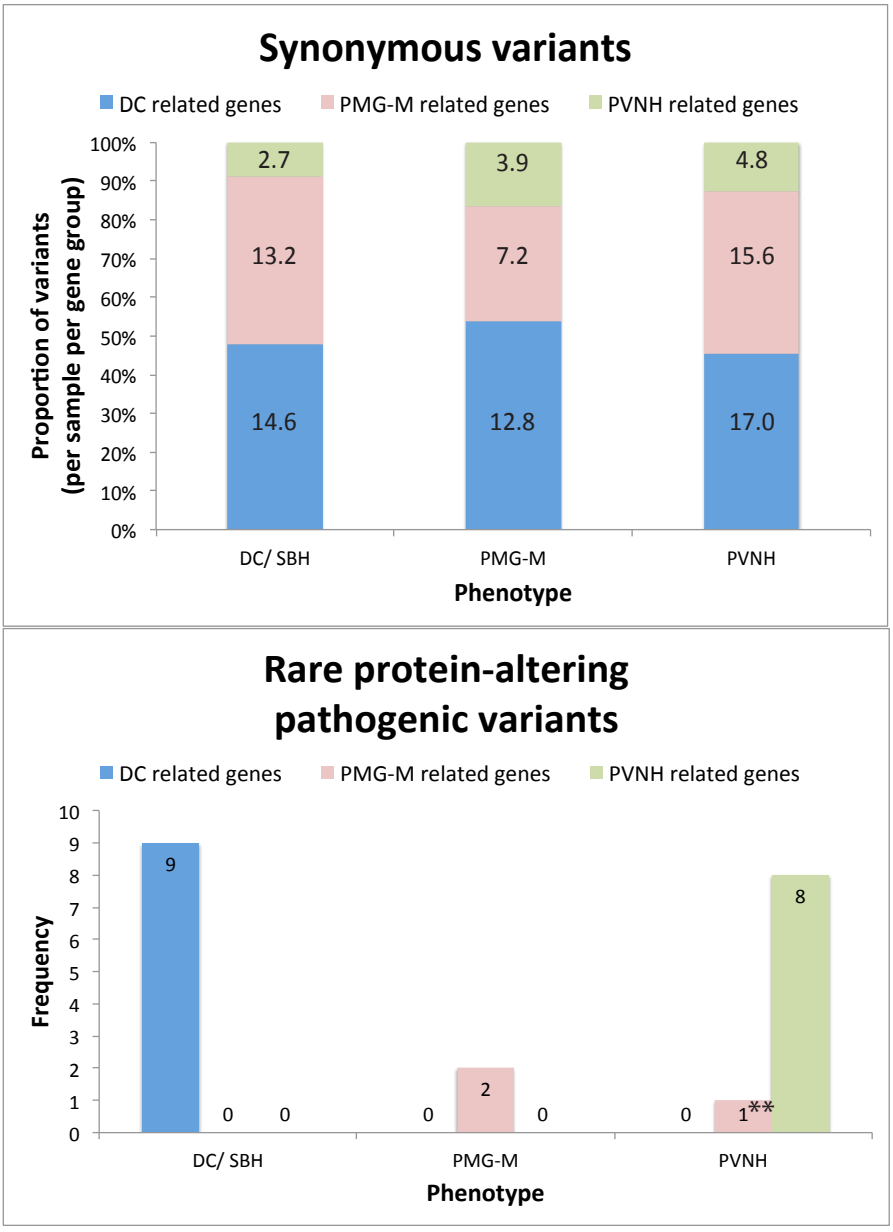

Figure S6: Spectrum of severity of doublecortex in mosaic individuals.
Axial MR images of the individuals with mosaicism (A-D) show a spectrum of the severity of doublecortex- (A) small and incomplete posteriorly in DC-4601, to (B) asymmetrical and more severe on the left hemisphere in DC-5103, to (C) complete but thin in DC-2101 to (D) full blown in DC-2801. (E) represents doublecortex as seen in DC-601, an individual with germline *DCX* mutation.

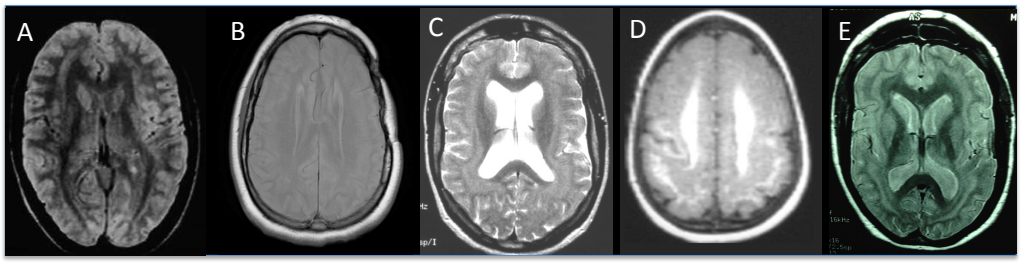

Figure S7: Axial and midline sagittal MRI brain of individual LIS-6801
MRI images show posterior pachygyria, diminished white matter volume and abnormal corpus callosum

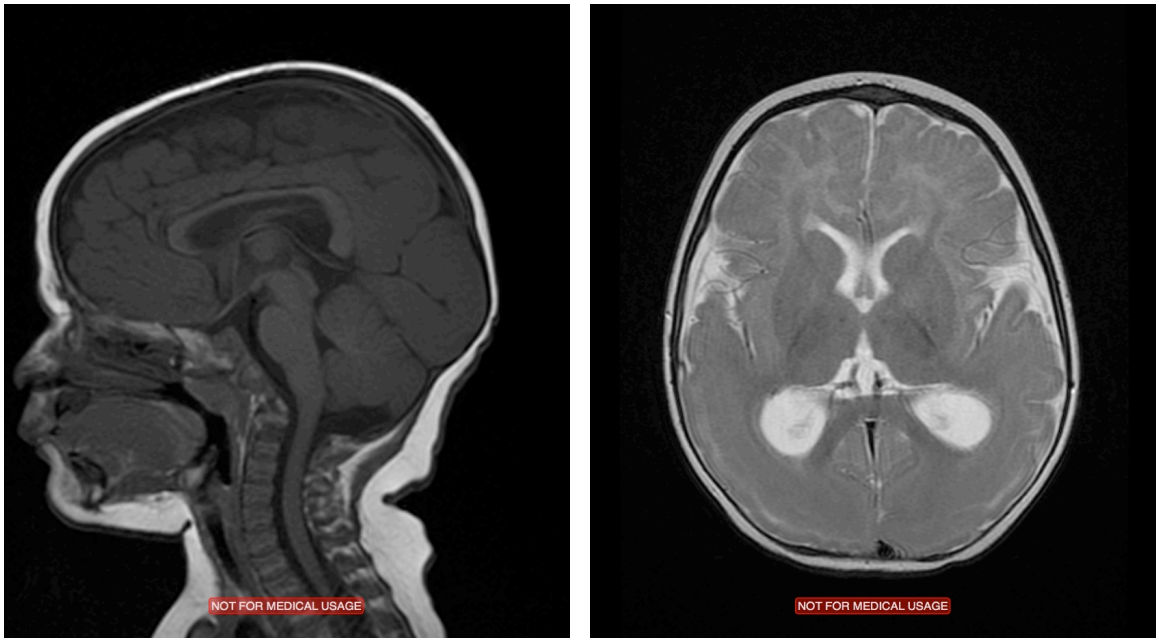

Figure S8: Sanger chromatogram of family BFP-801
Sanger chromatogram shows that the proband is heterozygous for the KIF7 variant (c.281C>T;pG94D) and her father is mosaic for the same variant. Mosaicism was confirmed on subcloning (not shown).

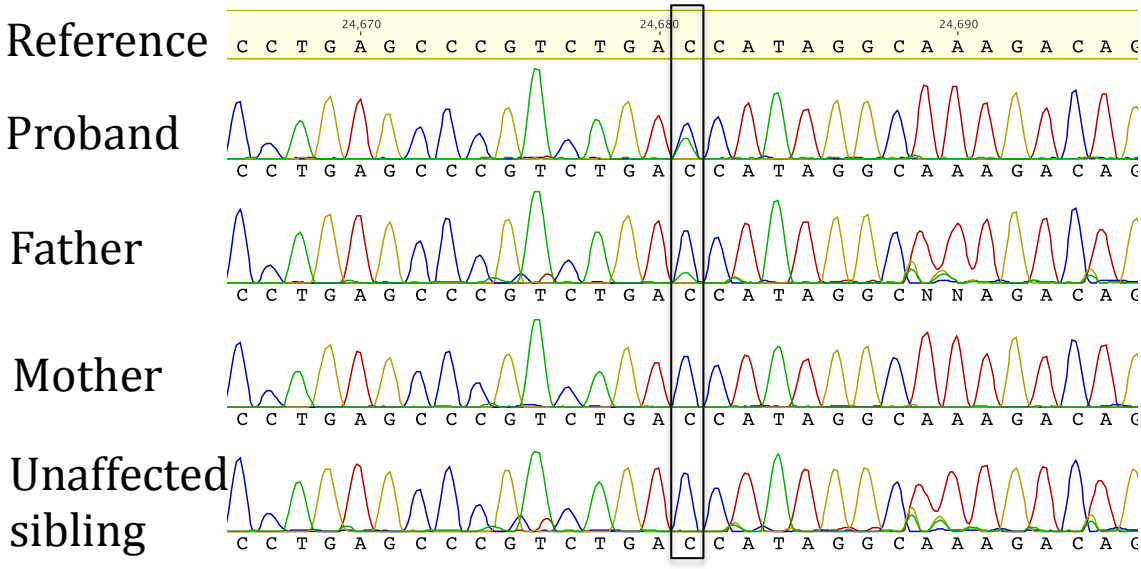

Figure S9: Axial and midline sagittal MRI brain of individual PAC-1701
MRI images show frontal pachygyria, diminished white matter volume and thick corpus callosum

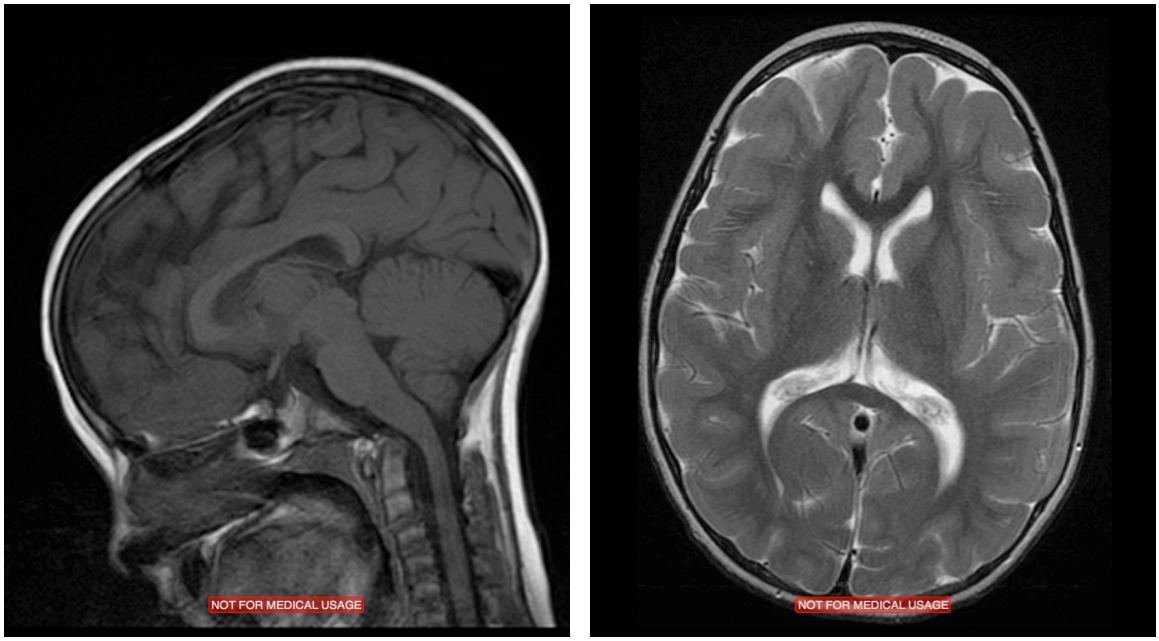

Figure S10: Axial MRI brain of individual DC-7801
MRI images show subcortical band heterotopia

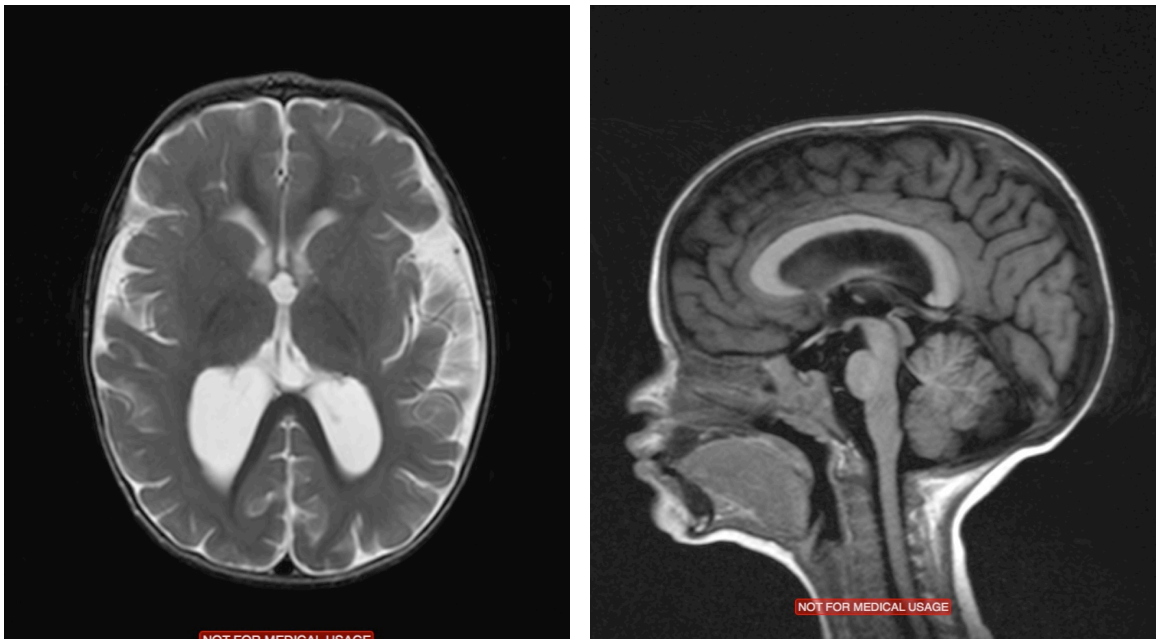

Table S1: List of known genes in the two panels

PANEL 1

Cumulative target (bp): 84,868

Coverage: 97%

Known genes:

Doublecortex/ pachygyria: *DCX, LIS1, ARX, TUBA1A, TUBB2B, TUBB3*

Periventricular nodular heterotopia: *FLNA*

Polymicrogyria with megalencephaly: *AKT3, PIK3CA, PIK3R2*

PANEL 2

Cumulative target (bp): 233,146

Coverage: 86%

Known genes:

Doublecortex/ pachygyria: *DCX, LIS1, ARX, TUBA1A, TUBB2B, TUBB3, ACTB, ACTG1*

Polymicrogyria with megalencephaly: *AKT3, PIK3CA, PIK3R2*

Cortical Malformations, recessive genes: *RELN, VLDLR, WDR62, NDE1*

Others: *DYNC1H1, KIF5C, TUBB4*

Table S2: Control samples

Gene	Genomic coordinate: nucleotide change	Protein alteration
AKT3 (mosaic)	chr1:243859016:C>T	E17K
DCX (mosaic)	chrX:110644295:C>A	V210F
DCX (germline)	chrX:110644345:T>A	K193M
DCX (germline)*	chrX:110653512:G>A	R39X
FLNA (germline)*	chrX:153599403:G>C	L71V

***used to generate mosaic control samples**

Table S3: Clinical phenotype of mutation positive patients

Sample ID	Gender	Ethnicity	Clinical info
DC-4601	Female	White/Non-Hispanic	Seizures onset 8years, atypical absence and focal seizures. Drug resistant. Normal development prior to onset of seizures
DC-4401	Male	White/Non-Hispanic	Not available
DC-2101	Female	White/Non-Hispanic	Intractable seizures. Right hemispherectomy performed in 2001
DC-5601	Female	White/Non-Hispanic	Not available
DC-601	Female	White/Non-Hispanic	Seizures onset 15 years, learning difficulties, mild ataxia
DC-7502	Female	Other/Unknown	Seizures at 3.5 yrs old. Delayed motor & speech development; head circumference at age 10y8m=53.5cm (78th%ile), maternal half sister with learning problems
LIS-5501	Female	White/Non-Hispanic	Not available
LIS-8401	Female	White/Non-Hispanic	Tongue tie, torticollis, multiple hemangiomas, gross motor delay, hypotonia, strabismus
DC-401	Female	White/Non-Hispanic	Intractable seizures necessitating temporal lobectomy, language delay and memory impairment
DC-5103	Female	White/Non-Hispanic	Febrile seizures at 13 months. Status epilepticus at 22 months. Subsequently, she had refractory epilepsy with complex partial seizures, developmental delay, as well as behavioral difficulties with hyperactivity and low attention span.
DC-2801	Female	White/Non-Hispanic	Severe seizures onset 2.5, severe intellectual disability motor delay.
PAC-101	Male	White/Non-Hispanic	Language and speech delays, fine motor skill delays, history of partial complex seizures
PAC-902	Male	White/Non-Hispanic	Seizure onset 2 days old- poorly controlled. Severe developmental delay, intellectual disability, and hypotonia. From age 7 years, noted to be dystonic with increased tone and multiple respiratory infections. Deceased at age 8.
PAC-1101	Female	White/Non-Hispanic	Developmental delay, possible seizures
LIS-6801	Female	White/Non-Hispanic	Infantile spasms at 6 months old. Developmental delay, increased tone. Prenatal evaluation was normal
PH-16001	Female	White/Non-Hispanic	Chronic lung disease, seizures, pulmonary hypertension, developmental delay, hypotonia, patent foramen ovale, VSD, small ASD, failure to thrive, thrombocytopenia, large platelets
DC-6302	Female	White/Non-Hispanic	Seizure onset at 15 years old, mostly controlled on Lamictal. Normal cognition and development.

PH-1101	Female	Asian	Not available
PH-19202	Female	White/Non-Hispanic	Events starting at age 10 of hand numbness. Optic disk papilledema. No cardiac findings.
PH-3901	Female	White/Non-Hispanic	Cleft palate, PDA post ligation at 3 months, intractable partial seizures with secondary generalization tonic/clonic seizures. At age 5, developmental delay.
PH-4801	Female	White/Non-Hispanic	Epilepsy onset 13yr, noted as well controlled at age 23 but worsening at age 27. Echocardiogram showed congenitally malformed, nonstenotic aortic valve (bicuspid aortic valve), mild aortic insufficiency. Seen for heart palpitations, right atrial enlargement and easy bruising
PH-4802	Female	White/Non-Hispanic	Prenatal hydrocephalus (HC 98%ile), severe developmental delay, abnormal eye movements, diffuse profound hypotonia, difficult seizures initially, controlled by age 2.5yr, chronic constipation, bilateral pes planovalgus, knee recurvatum and hip dysplasia
PH-8301	Male	White/Non-Hispanic	Onset of epilepsy at 17 years
PMG-3801	Male	White/Non-Hispanic	Macrocephaly (head circumference +4 SD). No skin findings. Died of pneumonia/ respiratory failure
PMG-14201	Male	White/Non-Hispanic	Not available
BFP-601	Male	Turkish	Seizures onset 5 years, mental and motor retardation
PMG-17401	Male	Hispanic	Dysarthria, cognitive delay, Head circumference 53 cm (~50%ile), normal vision and hearing, no seizures
PAC-1701	Female	White/Non-Hispanic	Developmental delay, ADHD, left eye strabismus, external rotation of right leg
DC-7801	Male	White/Non-Hispanic	Intractable seizures, infantile spasms, growth hormone deficiency, post axial polydactyly
BFP-801	Female	Turkish	Developmental delay by 10 months. No history of seizures. Mild right hemiparesis and increased tone.

Table S4: MRI report of mutation positive patients

Sample ID	MRI	Gene	Phenotype consistent with identified gene
DC-4601	Relatively mild subcortical band heterotopia with anterior to posterior gradient	*DCX*	Yes but milder
DC-4401	Subcortical band heterotopia	*DCX*	Yes
DC-2101	Subcortical band heterotopia. Thin outer cortical layer has slightly shallow sulci. Deeper cortical layer (the "band") is rather thin, ranging from 3 mm to 10 mm. Bilateral second, deeper (periventricular) foci of heterotopia measuring 2-3 mm x 5 mm are seen bilaterally between anterior aspect of ventricular trigone and the band.	*DCX*	Yes but milder
DC-5601	Subcortical band heterotopia	*DCX*	Yes
DC-601	Subcortical band heterotopia; atrophic cortex with small gyri/ enlarged sulci. Surrounding subarachnoid spaces are enlarged	*DCX*	Yes
DC-7502	Subcortical band heterotopia; cortex has normal thickness and normal number of sulci, slightly shallow, band involves most cerebrum with sparing of anterior and inferomedial temporal lobes, medial parietal and occipital lobes. Normal corpus callosum, cerebellum	*DCX*	Yes
LIS-5501	Classical lissencephaly. Hypogenic corpus callosum, hypoplastic cerebellar hemispheres and vermis.	*DCX*	Yes
LIS-8401	Classic lissencephaly with cell sparse zone, most severe in frontal lobes and least severe in parietal and occipital lobes.	*DCX*	Yes
DC-401	Subcortical band heterotopia	*LIS1*	Yes
DC-5103	Subcortical band heterotopia involving the occipital, temporal and parietal lobes and partially the frontal lobes of both hemispheres	*LIS1*	Yes, consistent with mosaic *LIS1*
DC-2801	Diffuse, severe band heterotopia in the posterior region, pachygyria in the anterior portions where the band is not recognizable. Moderate ventriculomegaly.	*LIS1*	Yes, consistent with mosaic *LIS1*
PAC-101	Posterior pachygyria, thick cortex with too few sulci in parietal lobes, extending partly into occipital lobes, absent rostrum, grossly normal white matter volume	*LIS1*	Yes
PAC-902	Frontal pachygyria, parietal, occipital and temporal polymicrogyria, a small dysplastic cerebellum, hypoplastic pons, and hypoplastic optic nerves	*TUBB2B*	Yes
PAC-1101	Periventricular nodular heterotopia- parietal pachygyria, globular hippocampi bilaterally, abnormally thick splenium of corpus callosum, diminished white matter	*TUBA1A*	Yes
LIS-6801	Posterior pachygyria with cell sparse zone involving posterior temporal lobes, parietal lobes, occipital lobes, frontal lobes normal, diminished white matter, abnormal corpus callosum (flat body long	*KIF5C*	NA

	splenium)		
PH-16001	Periventricular nodular heterotopia, heterotopia at variable size lining entirety of lateral ventricles, but not continuous, large right lateral ventricle, slightly reduced white matter volume	*FLNA*	Yes
DC-6302	Bilateral periventricular nodular heterotopia	*FLNA*	Yes
PH-1101	Periventricular nodular heterotopia	*FLNA*	Yes
PH-19202	Extensive subependymal heterotopia with mild supratentorial volume loss for age.	*FLNA*	Yes
PH-3901	Periventricular heterotopia	*FLNA*	Yes
PH-4801	Extensive areas of heterotopia along margins of lateral ventricles.	*FLNA*	Yes
PH-4802	Periventricular nodular heterotopia, small heterotopia lining nearly the entirety of the lateral ventricles, cortex appears normal but incompletely evaluated, fully formed corpus callosum, thinned by hydrocephalus, white matter volume reduced	*FLNA*	Yes
PH-8301	Unilateral nodular heterotopia (not contiguous)	*FLNA*	Yes
PMG-3801	Near generalized polymicrogyria and macrocephaly	*AKT3*	Yes
PMG-14201	Bilateral perisylvian polymicrogyria. Delicate polymicrogyria centered in sylvian fissures, involving most of frontal, parietal, and temporal lobes. Excessive folding of calcarine cortex bilaterally.	*PIK3CA*	Yes
BFP-601	Pachygyria with anterior-posterior gradient (worse posteriorly). Broad gyri, shallow sulci, thick cortex. Worst in parietal lobes. Least severe in anterior frontal and temporal lobes. Absent rostrum, small splenium	*DYNC1H1*	Yes
PMG-17401	Pachygyria, thick gyri and cortex in posterior frontal parietal and occipital lobes, shallow sulci, no cell-sparse zone seen, small PVNH in left trigone, absent inferior genu, rostrum of corpus callosum	*DYNC1H1*	Yes
PAC-1701	Mild pachygyria mildly thickened cortex with reduced number of sulci less severe in occipital than frontal lobes, body and splenium of corpus callosum are too thin, mild-mod white matter reduction	*KIF1A*	NA
DC-7801	Posterior subcortical band heterotopia with pachygyria anteriorly. Thick corpus callosum.	*KIF26A*	NA
BFP-801	Bilateral frontal, temporal, and parietal pachygyria	*KIF7*	NA

Table S5: Details of germline mutations (pathogenic and variants of uncertain significance)

Phenotype	Patient ID	Gender	Gene	Variant	Protein	SIFT	Polyphen-2
DC/SBH	DC-7502	Female	*DCX*	ChrX:110644560:A>G	Splicing	-	-
DC/SBH	DC-5601[1]	Female	*DCX*	ChrX:110644444:delA	Frameshift	-	-
DC/SBH	DC-601[1]	Female	*DCX*	ChrX:110644367:C>T	R186C	Deleterious	Probably damaging
PAC	LIS-5501	Female	*DCX*	ChrX:110653451:G>A	R59H	Deleterious	Probably damaging
PAC	LIS-8401	Female	*DCX*	ChrX:110576302:A>G	D343G	Deleterious	Probably damaging
PAC	BFP-601	Male	*DYNC1H1*	Chr14:102452244:A>G	E561G	Deleterious	Probably damaging
PAC	PMG-17401	Male	*DYNC1H1*	Chr14:102498756:G>A	R3344Q	Deleterious	Probably damaging
PAC	PAC-1101	Female	*TUBA1A*	Chr12:49578924:G>A	V409I	Deleterious	Benign
PAC	PAC-101	Male	*LIS1*	Chr17:2573541:G>A	G162S	Tolerated	Probably damaging
PAC	LIS-6801[1]	Female	*KIF5C*	Chr2:149806440:G>T	A268S	Deleterious	Possibly damaging
PMG-M	PMG-3801	Male	*AKT3*	Chr1:243668598:C>T	R465W	Deleterious	Probably damaging
PMG-M	PMG-14201[1]	Male	*PIK3CA*	Chr3:178952049:C>T	A1035V	Deleterious	Probably damaging
PVNH	DC-6302	Female	*FLNA*	ChrX:152591047:delC	C796Afs	-	-
PVNH	PH-1101[2]	Female	*FLNA*	ChrX:153590679:C>T	R863X	-	-
PVNH	PH-19202[2]	Female	*FLNA*	ChrX:153580926:insT	E2160X	-	-
PVNH	PH-3901	Female	*FLNA*	ChrX:153583416_153583419:delTGAA	I1656Rfs	-	-

PVNH	PH-4801[2]	Female	*FLNA*	ChrX:153592478:insA	Y731X	-	-
PVNH	PH-4802[2]	Female	*FLNA*	ChrX:153592478:insA	Y731X		
PVNH	PH-8301[1]	Male	*FLNA*	ChrX:153592950:C>T	L656F	Tolerated	Possibly damaging
Variants of uncertain significance							
DC/SBH	DC-7801	Male	*KIF26A*	Chr14:104638949	Q455R	Tolerated	Probably damaging
PAC	BFP-801[3]	Female	*KIF7*	Chr15:90195881	G94D	Deleterious	Probably damaging
PAC	PAC-1701[1]	Female	*KIF1A*	Chr2:241737118	R18W	Deleterious	Probably damaging

[1]Samples for which parental DNA was unavailable

[2]Multiple affected individuals within the family - variant segregated with the phenotype

[3]Inherited from father who is mosaic for the variant

Table S6: Protein-altering variants predicted to be non-pathogenic by *in silico* prediction algorithms

Patient ID	Gene	Variant	cDNA	Protein	SIFT	Polyphen	Comments
PS-6101	*FLNA*	chrX:153588202	3877G>A	V1293I	Tolerated	Benign	Parental DNA unavailable
PH-16303	*mTOR*	Chr1:11188128	5966A>G	I1989T	Tolerated	Benign	Parental DNA unavailable
PH-18001	*mTOR*	Chr:11184586	6631A>G	N2211D	Tolerated	Benign	Parental DNA unavailable
DC-2801	*KIF18A*	Chr11:28119200	295C>A	R99S	Tolerated	Benign	Parental DNA unavailable
MR-1401	*KIF21B*	Chr1:200977938	406G>A	V136M	Tolerated	Benign	Parental DNA unavailable

Table S7: Inherited variants- detected in unaffected parent and/or unaffected sibling

Patient ID	Gene	Variant	cDNA	Protein	SIFT	Polyphen	Comments
DC-7401	*KIF3B*	Chr20:30898442	862A>C	T288P	Deleterious	Benign	Inherited
LIS-5701	*KIF3B*	Chr20:30897624	44G>A	R15H	Deleterious	Probably damaging	Inherited
LIS-6001	*DYNC1I2*	Chr2:172600647	1625G>A	C542Y	Deleterious	Probably damaging	Inherited
PAC-2201	*DYNC1I2*	Chr2:172604320	1838G>A	R613Q	Deleterious	Benign	Inherited
LIS-8301	*KIF5A*	Chr12:57957244	152G>A	R51H	Deleterious	Benign	Inherited
PAC-601	*KIF22*	Chr16:29810622	797G>A	R266Q	Tolerated	Possibly damaging	Inherited
PAC-601	*NUDC*	Chr1:27269428	613C>T	R205W	Deleterious	Benign	Inherited
PH-23901	*PIK3R2*	Chr19:18272181	691C>T	R231C	Deleterious	Possibly damaging	Inherited

PMG-8401	*PAX6*	Chr11:31812317	1124C>A	P375Q	Deleterious	Possibly damaging	Inherited
PMG-17401	*VLDLR*	Chr9:2648672	1966C>T (het)	R656C	Deleterious	Probably damaging	Inherited/ carrier
DC-2201	*WDR62*	Chr19:36587931	2470C>T (het)	P824S	Tolerated	Possibly Damaging	Carrier

Table S8: *p* value for the AARF for each sample

Sample ID	Gene	Coverage	Minor allele count	% minor allele	*p* value*
Mosaic					
DC-4601	*DCX*	1981	90	5%	2.2e-226
DC-4401	*DCX*	2741	241	9%	8.3e-246
DC-401	*LIS1*	3020	394	13%	9.6e-210
DC-2101	*DCX*	555	85	15%	1.9e-32
DC-5103	*LIS1*	1400	221	16%	1.0e-82
PAC-902	*TUBB2B*	1290	301	23%	7.3e-45
DC-2801	*LIS1*	1456	384	26%	2.5e-39
PH-16001	*FLNA*	1032	362	35%	7.1e-12
Germline					
PMG-3801	*AKT3*	514	243	47%	0.38
DC-5601	*DCX*	971	451	46%	0.12
DC-601	*DCX*	1803	922	51%	0.49

DC-7502	*DCX*	1270	622	49%	0.61
LIS-5501	*DCX*	1022	497	49%	0.53
LIS-8401	*DCX*	453	213	47%	0.36
BFP-601	*DYNC1H1*	958	478	50%	0.96
PMG-17401	*DYNC1H1*	490	239	49%	0.70
DC-6302	*FLNA*	378	194	51%	0.72
PH-1101	*FLNA*	407	165	41%	0.007**
PH-19202	*FLNA*	294	128	44%	0.12
PH-3901	*FLNA*	114	49	43%	0.29
PH-4801	*FLNA*	316	170	54%	0.34
PH-4802	*FLNA*	444	225	51%	0.84
PH-8301	*FLNA*	61	61	100%	NA
LIS-6801	*KIF5C*	221	141	64%	0.003**
PAC-101	*LIS1*	639	277	43%	0.017**
PMG-14201	*PIK3CA*	1572	749	48%	0.19

PAC-1101	*TUBA1A*	383	185	48%	0.64

*Chi square test

**topocloning confirmed that these variants were germline

Table S9: Comparison of proportion of reads with mosaic variant detected on NGS and subcloning for validated and not validated variants

Variants that validated were detected at a coverage of ≥ 100x

Sample ID	Gene	Coverage	% of reads with alternate allele	Number of clones sequenced	% of clones with alternate allele	*p* value
DC-4601	*DCX*	1981	5%	84	2%	NS
DC-4401	*DCX*	2741	9%	40	10%	NS
DC-401	*LIS1*	3020	13%	116	10%	NS
DC-2101	*DCX*	555	15%	40	15%	NS
DC-5103	*LIS1*	1400	16%	17	12%	NS
PAC-902	*TUBB2B*	1290	23%	37	27%	NS
DC-2801	*LIS1*	1456	26%	37	22%	NS
PH-16001	*FLNA*	1032	35%	185	36%	NS

Variants that did not validate were detected at a coverage of ≤ 60x

Sample ID	Gene	Coverage	% of reads with	Number of clones	% of clones with	*p* value

			alternate allele	**sequenced[1]**	**alternate allele**	
PS-6101[2]	*PIK3R2*	20	20%	13	0	0.12
PS-6101[2]	*TSC1*	30	20%	0	0	-
SE-2401	*TUBB6*	18	22%	12	0	0.05
PS-6101	*PIK3R2*	23	22%	24	0	0.03
BFP-601	*KIF7*	17	24%	40	0	0.004
PMG-11301	*TUBB2A*	60	25%	20	0	0.01
PAC-701	*KIF26A*	20	25%	15	0	0.05
LIS-5901	*KIF26A*	10	40%	13	0	0.02

[1]Adequate numbers were sequenced for each non-validated variant to obtain a p-value of <0.05 reflecting that the variant was likely a sequencing error

[2]DNA was unavailable for further subcloning experiments

NS= not significant

Table S10: Details of the mosaic mutations detected by our panel

Sample ID	Gene	Type of mutation (cDNA/protein)	Remarks
DC-4601	*DCX*	Missense (R186C)	Moderately conserved nucleotide, highly conserved amino acid, in the doublecortin domain
DC-4401	*DCX*	Missense (R78L)	Highly conserved nucleotide and amino acid, in the doublecortin domain
DC-401	*LIS1*	Nonsense (K64X)	Premature stop codon. Present at 35% in buccal derived DNA and 23% in saliva derived DNA
DC-2101	*DCX*	Splicing (1270-1G>A)	Skip of exon 7, which may lead to an abnormally folded protein or an unstable mRNA
DC-5103	*LIS1*	Missense (R342P)	Highly conserved nucleotide and amino acid, in WD40 repeat
PAC-902	*TUBB2B*	Missense (R380P)	Moderately conserved nucleotide, highly conserved amino acid, in the tubulin domain
DC-2801	*LIS1*	Splicing (1002+1G>A)	Skip of exon 9
PH-16001	*FLNA*	Frameshift (S1449Pfs*10)	Creates a frameshift starting at codon Ser 1449, new reading frame ends in a stop codon 9 positions downstream

Table S11: Further details of the reported mutations

Phenotype	Patient ID	Gene	Variant	Germline VS mosaic	Type of mutation	Previously reported
DC/SBH	DC-4601	*DCX*	ChrX:110644367:C>T	Mosaic (5%)	Missense	Yes[16,17]
DC/SBH	DC-4401	*DCX*	ChrX:110653322:G>T	Mosaic (9%)	Missense	Yes[17,18]
DC/SBH	DC-2801	*LIS1*	Chr17:2579901:G>A	Mosaic (26%)	Splicing	Yes[19]
PAC	PAC-902	*TUBB2B*	Chr6:3225184:G>C	Mosaic (23%)	Missense	Yes[20]
DC/SBH	DC-7502	*DCX*	ChrX:110644560:A>G	Germline	Splicing	Yes[16]
DC/SBH	DC-601	*DCX*	ChrX:110644367:C>T	Germline	Missense	Yes[16,17]
PAC	LIS-5501	*DCX*	ChrX:110653451:G>A	Germline	Missense	Yes[21,22]
PAC	PMG-17401	*DYNC1H1*	Chr14:102498756:G>A	Germline	Missense	Yes[10]
PAC	PAC-101	*LIS1*	Chr17:2573541:G>A	Germline	Missense	Yes[19,23]
PMG-M	PMG-3801	*AKT3*	Chr1:243668598:C>T	Germline	Missense	Yes[24]
PMG-M	PMG-14201	*PIK3CA*	Chr3:178952049:C>T	Germline	Missense	Yes[24]
PVNH	PH-8301	*FLNA*	ChrX:153592950:C>T	Germline	Missense	Yes[25]
DC/SBH	DC-2101	*DCX*	ChrX:110544972:G>A	Mosaic (15%)	Splicing	No
DC/SBH	DC-401	*LIS1*	Chr17:2569382:A>T	Mosaic (13%)	Nonsense	No
PVNH	PH-1101	*FLNA*	ChrX:153590679:C>T	Germline	Nonsense	No

DC/SBH	DC-5601	*DCX*	ChrX:110644444:delA	Germline	Frameshift	No
PVNH	PH-16001	*FLNA*	ChrX:153587482:delG	Mosaic (35%)	Frameshift	No
PVNH	DC-6302	*FLNA*	ChrX:152591047:delC	Germline	Frameshift	No
PVNH	PH-19202	*FLNA*	ChrX:153580926:insT	Germline	Frameshift	No
PVNH	PH-3901	*FLNA*	ChrX:153583416_ 153583419:delTGAA	Germline	Frameshift	No
PVNH	PH-4801	*FLNA*	ChrX:153592478:insA	Germline	Frameshift	No
PVNH	PH-4802	*FLNA*	ChrX:153592478:insA	Germline	Frameshift	No
DC/SBH	DC-5103	*LIS1*	Chr17:2583480:G>C	Mosaic (16%)	Missense	No
PAC	LIS-8401	*DCX*	ChrX:110576302:A>G	Germline	Missense	No
PAC	BFP-601	*DYNC1H1*	Chr14:102452244:A>G	Germline	Missense	No
PAC	PAC-1101	*TUBA1A*	Chr12:49578924:G>A	Germline	Missense	No
PAC	LIS-6801	*KIF5C*	Chr2:149806440:G>T	Germline	Missense	No

Table S12: **Summary of MRI findings of individuals with de novo variants in *DYNC1H1***

Patient ID	**Mutation**		**MRI**				
	gDNA	Protein	Cortex	Corpus Callosum	Brainstem	Cerebellum	Others
BFP-601	14:102452244A>G	E561G	Pachygyria with A-P gradient (worse posteriorly)	Absent rostrum, small splenium	Normal	Normal	Mild enlargement of trigones
PMG-17401	14:102498756G>A	R3344Q	Pachygyria in the posterior frontal, parietal and occipital lobes	Absent rostrum and inferior genu	Normal	Normal	Small heterotopia in left trigone
LIS-8201	14:102446852G>A	R309H	Posterior pachygyria with cell sparse zone	Small inferior genu, small splenium	Short pons	Small anterior vermis	Small olfactory bulbs, prominent perivascular spaces
PAC-1601	14:102452268G>C	R569P	Posterior pachygyria with cell sparse zone	Absent rostrum, mildly enlarged ventricles	Normal	Normal	Decreased white matter volume

SUPPLEMENTARY REFERENCES

1. Fietz SA, Lachmann R, Brandl H, et al. Transcriptomes of germinal zones of human and mouse fetal neocortex suggest a role of extracellular matrix in progenitor self-renewal. Proc Natl Acad Sci U S A 2012;109:11836-41.

2. Li H, Durbin R. Fast and accurate long-read alignment with Burrows-Wheeler transform. Bioinformatics 2010;26:589-95.

3. McKenna A, Hanna M, Banks E, et al. The Genome Analysis Toolkit: a MapReduce framework for analyzing next-generation DNA sequencing data. Genome Res 2010;20:1297-303.

4. Illumina Technical Note: Somatic Variant Caller (URL: http://res.illumina.com/documents/products/technotes/technote_somatic_variant_caller.pdf) [July, 2013].

5. Exome Variant Server, NHLBI Exome Sequencing Project (ESP), Seattle, WA (URL: http://evs.gs.washington.edu/EVS/) [September, 2013].

6. Sherry ST, Ward MH, Kholodov M, et al. dbSNP: the NCBI database of genetic variation. Nucleic Acids Res 2001;29:308-11.

7. Abecasis GR, Auton A, Brooks LD, et al. An integrated map of genetic variation from 1,092 human genomes. Nature 2012;491:56-65.

8. Ng PC, Henikoff S. Predicting deleterious amino acid substitutions. Genome Res 2001;11:863-74.

9. Adzhubei IA, Schmidt S, Peshkin L, et al. A method and server for predicting damaging missense mutations. Nat Methods 2010;7:248-9.

10. Poirier K, Lebrun N, Broix L, et al. Mutations in TUBG1, DYNC1H1, KIF5C and KIF2A cause malformations of cortical development and microcephaly. Nat Genet 2013;45:639-47.

11. Dafinger C, Liebau MC, Elsayed SM, et al. Mutations in KIF7 link Joubert syndrome with Sonic Hedgehog signaling and microtubule dynamics. J Clin Invest 2011;121:2662-7.

12. Putoux A, Thomas S, Coene KL, et al. KIF7 mutations cause fetal hydrolethalus and acrocallosal syndromes. Nat Genet 2011;43:601-6.

13. Liu JS, Schubert CR, Fu X, et al. Molecular basis for specific regulation of neuronal kinesin-3 motors by doublecortin family proteins. Mol Cell 2012;47:707-21.

14. Hamdan FF, Gauthier J, Araki Y, et al. Excess of de novo deleterious mutations in genes associated with glutamatergic systems in nonsyndromic intellectual disability. Am J Hum Genet 2011;88:306-16.

15. Zhou R, Niwa S, Homma N, Takei Y, Hirokawa N. KIF26A is an unconventional kinesin and regulates GDNF-Ret signaling in enteric neuronal development. Cell 2009;139:802-13.

16. des Portes V, Francis F, Pinard JM, et al. doublecortin is the major gene causing X-linked subcortical laminar heterotopia (SCLH). Hum Mol Genet 1998;7:1063-70.

17. Bahi-Buisson N, Souville I, Fourniol FJ, et al. New insights into genotype-phenotype correlations for the doublecortin-related lissencephaly spectrum. Brain 2013;136:223-44.

18. Pilz DT, Matsumoto N, Minnerath S, et al. LIS1 and XLIS (DCX) mutations cause most classical lissencephaly, but different patterns of malformation. Hum Mol Genet 1998;7:2029-37.

19. Cardoso C, Leventer RJ, Matsumoto N, et al. The location and type of mutation predict malformation severity in isolated lissencephaly caused by abnormalities within the LIS1 gene. Hum Mol Genet 2000;9:3019-28.

20. Cushion TD, Dobyns WB, Mullins JG, et al. Overlapping cortical malformations and mutations in TUBB2B and TUBA1A. Brain 2013;136:536-48.

21. Gleeson JG, Minnerath SR, Fox JW, et al. Characterization of mutations in the gene doublecortin in patients with double cortex syndrome. Ann Neurol 1999;45:146-53.

22. Matsumoto N, Leventer RJ, Kuc JA, et al. Mutation analysis of the DCX gene and genotype/phenotype correlation in subcortical band heterotopia. Eur J Hum Genet 2001;9:5-12.

23. Caspi M, Coquelle FM, Koifman C, et al. LIS1 missense mutations: variable phenotypes result from unpredictable alterations in biochemical and cellular properties. J Biol Chem 2003;278:38740-8.

24. Riviere JB, Mirzaa GM, O'Roak BJ, et al. De novo germline and postzygotic mutations in AKT3, PIK3R2 and PIK3CA cause a spectrum of related megalencephaly syndromes. Nat Genet 2012;44:934-40.

25. Sheen VL, Dixon PH, Fox JW, et al. Mutations in the X-linked filamin 1 gene cause periventricular nodular heterotopia in males as well as in females. Hum Mol Genet 2001;10:1775-83.